PROCEEDINGS OF SPIE

SPIEDigitalLibrary.org/conference-proceedings-of-spie

Computational analysis of cerebrovascular structures imaged using two-photon microscopy

Siddhartha Dhiman, Itender Singh, Pinaki Sarder

Siddhartha Dhiman, Itender Singh, Pinaki Sarder, "Computational analysis of cerebrovascular structures imaged using two-photon microscopy," Proc. SPIE 10956, Medical Imaging 2019: Digital Pathology, 1095617 (18 March 2019); doi: 10.1117/12.2513234

SPIE.

Event: SPIE Medical Imaging, 2019, San Diego, California, United States

Computational analysis of cerebrovascular structures imaged using two-photon microscopy

Siddhartha Dhiman[1], Itender Singh[2], and Pinaki Sarder[1]

[1]Departments of Pathology and Anatomical Sciences, University at Buffalo

[2]Department of Neurological Surgery, Washington University School of Medicine in St. Louis

[*]Address all correspondence to: Pinaki Sarder; Tel: 716-829-2265, E-mail: pinakisa@buffalo.edu

ABSTRACT

Neurodegenerative diseases including Alzheimer's affect millions around the world, and this number is projected to increase over the years unless a breakthrough is made. There are several theories on the pathogenesis of neurodegenerative diseases, with the amyloid cascade and tau theory being the most prominent ones. The formation of amyloid plaques and tau tangles collapses capillaries in the brain, thereby inducing hypoxia and destruction of neurons from loss of nourishment. While we do understand some of the changes that occur in the brain's vasculature form the pathogenesis of these diseases, they have not yet been mathematically characterized with precision. A computational pipeline is presented here to analyze optically sectioned mice brain sections imaged via two-photon microscopy and characterize various vasculature parameters which are known to deteriorate from neurogenerative diseases. Our proposed pipeline aims to quantify various brain vasculature parameters, such as, vessel tortuosity, diameter, volume and length, as well the degree of difference to understand disease pathogenesis with the eventual hope of providing drug intervention to regress or minimize these changes.

Keywords: Alzheimer's, Vasculature, Two-photon microscopy, Segmentation, Cerebrovascular, Amyloid cascade theory, Neurofibrillary tangles, Medical image processing

I. INTRODUCTION

Cerebrovascular impairment is a major contributor to later-life dementia after Alzheimer's Disease (AD)[1,2]. Vascular Dementia (VaD) is a condition in which cerebrovascular changes or deterioration lead to cognitive impairment, and eventually the onset of dementia[3]. While both VaD and AD are widely recognized to cause dementia, their pathogenesis differs. In contrast, AD is caused by accumulation of amyloid plaques and tau interlibrary tangles[3–5].

Medical Imaging 2019: Digital Pathology, edited by John E. Tomaszewski, Aaron D. Ward,
Proc. of SPIE Vol. 10956, 1095617 · © 2019 SPIE · CCC code:
1605-7422/19/$18 · doi: 10.1117/12.2513234

It has been hypothesized that toxic protein peptides amyloid-beta (A_β) and Tau cause noticeable changes and degeneration of blood vessel in the brain of an AD patient, which is correlated with the degree of dementia and permeability of the blood-brain-barrier (BBB) surrounding these regions[4,5], brain hypoperfusion[6], and endothelial cell death and collapse of capillaries[7,8]. This effect is more prominent in old ages where angiogenesis may fail and intensify the effects of hypoxia-stimulated vessel collapse[8].

VaD is more commonly associated with both large and small vessel infarcts[3], which can have several risk factors such as heart disease, diabetes, etc[3]. Of these risk factors, particularly important is type 2 diabetes mellitus (DM2), which has been shown to have strong correlation with dementia[9,10]. Variations in glucose, insulin, and amyloid metabolism can happen from onset of DM2. Furthermore, DM2 may affect vascular reactivity by advanced glycosylation end products, which could result in perfusion abnormalities[11].

Given bouts of cerebrovascular changes from the onset of AV, VaD, or any other neurodegenerating disease, we aim to develop a pipeline to characterize cerebral vasculature from two-photon microscopy. 3D images of vasculature can be obtained by either physically slicing a sample into multiple layers and stitching the image together or using optical sectioning. Physical slicing introduces distortion in a sample from the blade's compression and shear force. Optical sectioning technique such as two-photon microscopy used in this study focuses on different planes along the optical axis of the sample to create a 3D image. This pipeline will be applied on mice brains due to their ease of access; human samples are far more difficult to obtain. In addition, mice physiology closely resembles that of humans, gives researchers precise control over the disease model and various variables, and studies using mouse models will allow studying drug intervention strategies in a controlled fashion.

II. METHODS

Imaging and data preparation. Intact brain tissue sections from $n = 3$ normal mice were imaged via a two-photon microscope (Zeiss 510 Meta). Respective optical cross-sections of brain vasculature were obtained, where brain vasculature was targeted, and fluorescence light was generated. Image resolution was 512 x 512 per optical section, with number of optical sections varying from 204 to 257. X, Y and Z voxel sizes were 0.82 µm, 0.82 µm and 2.00 µm respectively. Images were then split into TIFF stacks and recombined to MATLAB object files.

Frangi vesselness filter. Image processing was initiated with the Frangi filter to compute regions that most likely contain vessels to enhance the image. Voxel anisotropy and noise often pose a problem in vessel segmentation[12]. Frangi vesselness filter overcomes most problems in 3D vasculature segmentation by searching for geometric structures with tube-like properties. Taking a 3D image as an input, this filter determines the eigenvectors of the image's Hessian to compute the vessel-likeliness of a region[13,14]. The output is a 3D image containing regions most likely to be a vessel. Here most noise and artifacts in images are removed to produce more isotropic voxels.

Layer-by-layer processing. Image processing was continued with top-hat filter to minimize uneven illumination and contrast-limited adaptive histogram equalization (CLAHE) to enhance contrast of vascular regions. The overall effect of the two filters greatly enhances contrast of vasculature-containing regions for thresholding. These operations were applied on a layer-by-layer basis down the optical sections. It was assumed the 3D images were isotropic with regards to features due to the application of Frangi filter.

3D filtering. 3D outputs of the above steps were further processed by 3 x 3 x 3 median and mean filters to minimize any remnant noise in image. The resulting images were near noise-free 3D images.

Otsu's thresholding. The resulting image was then binarized using this standard image segmentation technique. Otsu's method evaluates the separability of classes in bimodality of pixel intensity distribution[15], and is a standard segmentation feature in the Image Processing Toolbox. Successful segmentation binarized the image such that vasculature-containing voxels were assigned a value of '1' and '0' otherwise.

Image cleaning. Following thresholding, solid vessel regions containing 'holes' or breaks in uniformity were flood-filled. Any remnant noise or tiny 'blobs' least likely to be vessels were also removed by specifying a threshold value, under which such regions were removed. The resulting image was a binarized 3D image containing the vasculature structure.

Skeletonization. The image was then skeletonized to estimate the centerline of vasculature and provide a skeleton framework for calculations. MATLAB 2018a added the capability of 3D skeletonizing, which calculates the 3D medial axis skeleton of a 3D volume while preserving Euler number of image objects[16–18]. The output produced by this function is a 3D binary image where all objects in image are reduced to 1-voxel wide curved lines, which were then established at centerlines for vasculature.

Branchpoints and endpoints. Next, we computed the branch and end points of the skeletonized binary volume. Branch points are points in the skeleton where multiple branches meet, and end points are the tips of vessels. A 3 x 3 x 3 lookup matrix iterates along the X, Y, and Z planes of the image to search for these points. In terms of a lookup matrix, a branch point is defined as one that contains three "on" voxels and 24 "off" voxels. In addition, for an "on" voxel in the center of the lookup matrix, a validity of a branch point is confirmed when there are two other "on" voxels surrounding the central "on" voxel. In contrast, end points are defined by the presence of two "on" voxels and 25 "off voxels", where there is one other "on" voxel in the lookup matrix for an "on" voxel in the center. Discovering branch and end points is imperative to vasculature quantification because they define coordinates where individual vessels start and stop within an image.

Vasculature characterization. Earlier it was mentioned that increased vessel coiling is associated with dementia, so vessel tortuosity is one of the parameters used to characterize vasculature. In the most simplistic sense, tortuosity can be defined as the ratio of vessel path length to the Euclidean distance between its end points[19]. The Geodesic distance is the shortest distance between two points along a curved surface[20]. Perturbations in vessel coiling can affect their path length, thus making it important to succulently pick a distance transform that can capture these variations. MATLAB's Image Processing Toolbox was used to perform Geodesic and Euclidean distance transform on the vessels to quantify the two distances, and then divided to obtain the tortuosity.

Application of this computational pipeline on one of the images is shown in Figs. 1A-1E. The final processed image is a skeletonized vasculature (figure 1E) to compute branch and end points for characterization.

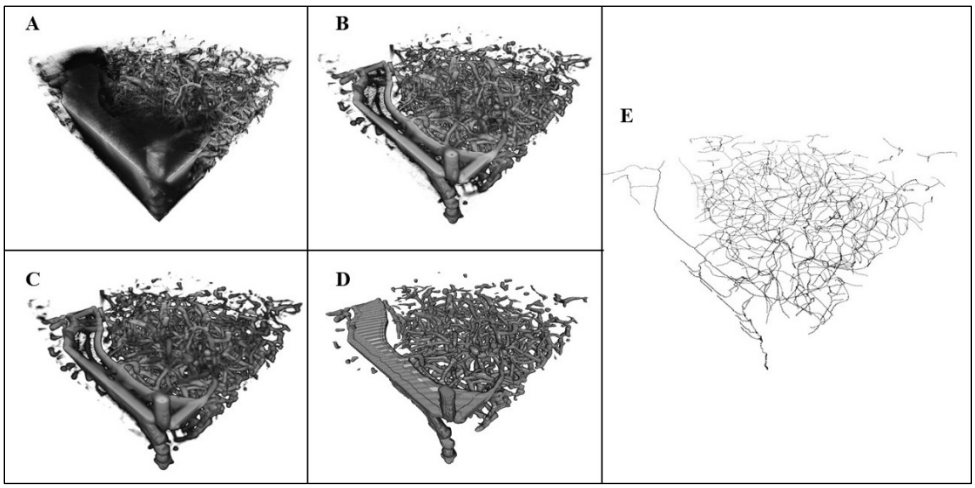

Figure 1. Steps of the proposed pipeline where A (top-left) shows the raw optically sectioned image containing vasculature. B (top-mid) shows the application of Frangi filter onto the raw image, following which the output of layer-by-layer processing and 3D filtering is shown in C (bottom-left). The image was then thresholded using Otsu's method, shown in D (bottom-mid). Skeletonization, as shown in E (right), was then obtained to estimate the vasculature's centerline for vessel parameterization.

III. RESULTS

Preliminary results analyzed from three healthy mice show a normally distributed tortuosity that varies minimally between samples; see Fig. 2. Healthy samples follow a certain distribution and variance in cerebrovascular tortuosity, and we hypothesize that this distribution is perturbed in diseased samples from hypoperfusion. We would expect a right-ward shift in the histograms in both AD and VaD samples as these diseases are characterized by increased coiling of vessels[21]. It is important to note that vessel tortuosity distribution among the three healthy mice closely resemble each other, indicative of a vessel coiling regulatory factor.

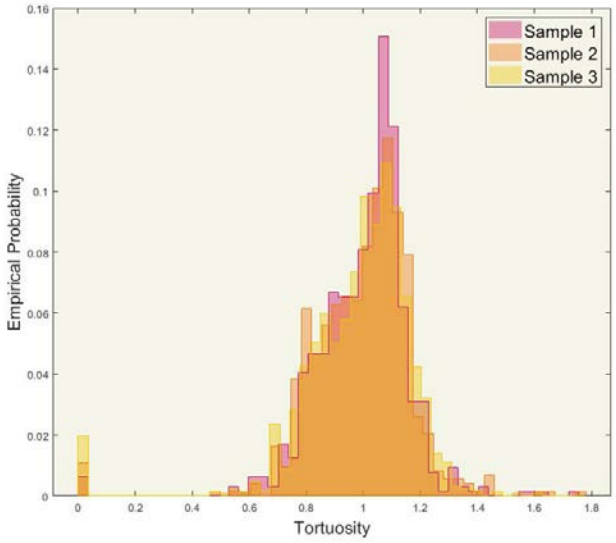

Figure 2. Distributions of tortuosity from three healthy mice. Preliminary results show that the distributions closely resemble each other, indicating that heathy mice demonstrate a specific range of vessel tortuosity.

IV. DISCUSSION

Segmentation of 3D vasculature often poses hurdles due to anisotropic nature of images and presence of noise. The Hessian-based Frangi filer allowed us to overcome the shortcomings of these images to maximize the preservation of vasculature post-segmentation. While one of the parameters to characterize vasculature has been completed, we aim to include additional parameters such as vessel diameter, volume and orientation in the final study because these factors are known to change from deposition of amyloid plaques and other risk cardiovascular and cerebrovascular risk factors. Literature review on this subject yielded almost no studies performed on the mathematical characterization of cerebrovascular changes resulting from neurodegenerating diseases, so there is a novelty to this study to precisely understand the pathogenesis of these diseases.

V. CONCLUSION AND FUTURE WORKS

This study aims to fill the whitespace in literature pertaining to mathematical characterization of cerebrovascular differences between healthy and neurological diseases with precision. The pipeline is potentially useful in achieving vessel segmentation and garnering knowledge on vasculature changes arising from various diseases. In the future, we intend to compare parameters between healthy and diseased mice models, in the hope of understanding the amyloid

cascade theory with greater depth. In addition, this pipeline can be applied to other diseases which cause cerebrovascular changes. In addition, we aim to apply this pipeline to different time points during the pathogenesis of Alzheimer's and DM2 to understand both the severity and degree of changes in the vasculature. This will shed more light on the development on dementia as it is already known that the severity of disease is correlated with the severity of amyloid plaques and tau tangles.

ACKNOWLEDGEMENT

The project was supported by the faculty startup funds from the Jacobs School of Medicine and Biomedical Sciences, University at Buffalo, and the University at Buffalo IMPACT award.

REFERENCES

[1] Erkinjuntti, T., "Cerebrovascular Dementia: Pathophysiology, Diagnosis and Treatment," CNS Drugs **12**(1), 35–48 (1999).
[2] Toledo, J. B., *et al.*, "Contribution of cerebrovascular disease in autopsy confirmed neurodegenerative disease cases in the National Alzheimer's Coordinating Centre," Brain **136**(9), 2697–2706 (2013).
[3] Kling, M. A., *et al.*, "Vascular disease and dementias: paradigm shifts to drive research in new directions," Alzheimers Dement. J. Alzheimers Assoc. **9**(1), 76–92 (2013).
[4] Wisniewski, H. M. and Kozlowski, P. B., "Evidence for Blood-Brain Barrier Changes in Senile Dementia of the Alzheimer Type (SDAT)," Ann. N. Y. Acad. Sci. **396**(1 Alzheimer's D), 119–129 (1982).
[5] Wisniewski, H. M., Vorbrodt, A. W. and Wegiel, J., "Amyloid Angiopathy and Blood?Brain Barrier Changes in Alzheimer's Disease [b]," Ann. N. Y. Acad. Sci. **826**(1 Cerebrovascul), 161–172 (1997).
[6] Weller, R. O., *et al.*, "Cerebral Amyloid Angiopathy," Am. J. Pathol. **153**(3), 725–733 (1998).
[7] Brown, W. R., "A Review of String Vessels or Collapsed, Empty Basement Membrane Tubes," J. Alzheimers Dis. **21**(3), 725–739 (2010).
[8] Brown, W. R. *et al.*, "Review: Cerebral microvascular pathology in ageing and neurodegeneration: Cerebral microvascular pathology," Neuropathol. Appl. Neurobiol. **37**(1), 56–74 (2011).
[9] Biessels, G. J., *et al.*, "Dementia and cognitive decline in type 2 diabetes and prediabetic stages: towards targeted interventions," Lancet Diabetes Endocrinol. **2**(3), 246–255 (2014).
[10] Stewart, R. and Liolitsa, D., "Type 2 diabetes mellitus, cognitive impairment and dementia," Diabet. Med. **16**(2), 93–112 (1999).
[11] Pasquier, F., *et al.*, "Diabetes mellitus and dementia," Diabetes Metab. **32**(5), 403–414 (2006).
[12] Orkisz, M. M., *et al.*, "Improved vessel visualization in MR angiography by nonlinear anisotropic filtering," Magn. Reson. Med. **37**(6), 914–919 (1997).
[13] Frangi, A. F., *et al.*, "Multiscale vessel enhancement filtering," [Medical Image Computing and Computer-Assisted Intervention — MICCAI'98], W. M. Wells, A. Colchester, and S. Delp, Eds., Springer Berlin Heidelberg, Berlin, Heidelberg, 130–137 (1998).
[14] "Hessian based Frangi Vesselness filter - File Exchange - MATLAB Central.", <https://www.mathworks.com/matlabcentral/fileexchange/24409> (6 August 2018).
[15] Otsu, N., "A Threshold Selection Method from Gray-Level Histograms," IEEE Trans. Syst. Man Cybern. **9**(1), 62–66 (1979).
[16] Lee, T. C., Kashyap, R. L. and Chu, C. N., "Building Skeleton Models via 3-D Medial Surface Axis Thinning Algorithms," CVGIP Graph. Models Image Process. **56**(6), 462–478 (1994).
[17] Kerschnitzki, M., *et al.*, "Architecture of the osteocyte network correlates with bone material quality: OSTEOCYTE NETWORK ARCHITECTURE CORRELATES WITH BONE MATERIAL QUALITY," J. Bone Miner. Res. **28**(8), 1837–1845 (2013).
[18] "Skeletonization - MATLAB & Simulink.", <https://www.mathworks.com/help/images/skeletonization.html> (10 August 2018).
[19] Shoelson, B., "Calculating arclengths…made easy!," File Exch. Pick Week (2012).

[20] Pokorny, P., “Geodesics Revisited,” Chaotic Model. Simul., 281–298 (2012).
[21] Buée, L., Hof, P. R. and Delacourte, A., “Brain microvascular changes in Alzheimer’s disease and other dementias,” Ann. N. Y. Acad. Sci. **826**, 7–24 (1997).